Velocity Variability in MRI Phase-Contrast

Ali Dehghan Firoozabadi[1], Pablo Irarrazaval[2, 3, 5], Sergio Uribe[3, 4], Cristian Tejos[2, 3], Carlos Sing-Long[3, 5, 6]

[1]Department of Electricity, Universidad Tecnologica Metropolitana, Av. Jose Pedro Alessandri 1242, Santiago, Chile
[2]Electrical Engineering Department, Pontificia Universidad Catolica de Chile, Santiago, Chile
[3]Biomedical Imaging Center, Pontificia Universidad Catolica de Chile, Santiago, Chile
[4]Radiology Department, School of Medicine, Pontificia Universidad Catolica de Chile, Santiago, Chile
[5]Institute for Biological and Medical Engineering, Pontificia Universidad Catolica de Chile, Santiago, Chile
[6]Institute for Mathematical and Computational Engineering, Pontificia Universidad Catolica de Chile, Santiago, Chile
E-mail: adehghanfirouzabadi@utem.cl

***Abstract*—MRI phase contrast is a well known technique for computing the average velocity associated to each pixel. In this work, we calculate the exact probability distribution function for the velocity given the noise in the signal. This pdf is not necessarily Gaussian, particularly for low Signal-to-Noise ratio. We first find the pdf of the signals phase, assuming Gaussian noise in the real and imaginary channels of the signal. The pdf of the velocity is then the convolution of the phases pdfs. To confirm this, we measure several times the velocity in a flow phantom and compare the empirical histogram with the theoretical pdf. We also acquire the velocity from a volunteers aorta using a standard protocol for 4D Flow and multiple coils. Based on this noise characterization, we also propose an optimal weighing for combining multiple coils which is not based only on the coil sensitivities.**

***Index Terms*—Flow MRI, Phase contrast velocity, Ascending and descending aorta**

I. Introduction

MRI Phase-Contrast [1] is a well known technique used to compute the velocity associated to each pixel. It assumes that all spins within the pixel have the same velocity (equivalently, it measures an average velocity) and that it is constant during the readout. These velocities are used in many applications such as MRI-PC Angiography [2], 4D Flow [3], quantization flow-rate [4], wall shear stress [5], [6], pressure [7], [8], and others.

For many of these applications it is necessary to know the precision and accuracy of the measured velocity. For example, if 4D Flow velocities are used to feed a fluid mechanic model to estimate physiologically important parameters, such as pressure, and others, one way to estimate the quality of the estimation is by knowing the precision of the input data (it turns out that accuracy is not a problem because there is no bias).

In most of the literature referring to the Velocity-to-Noise Ratio (VNR) [9]–[12] it is assumed that the standard deviation of the velocity is:

$$\sigma_V = \frac{\sqrt{2}}{\pi}\frac{V_{\text{enc}}}{\text{SNR}} \tag{1}$$

where V_{enc} is the maximum encoded velocity and SNR, the signal-to-noise ratio in the image. We will show that this is not necessarily true, first because the standard deviation is not the same for all pixels as stated in [13] and [14], and second, because this formula assumes a Gaussian distribution which is not true for low signal regions [15].

The purpose of this work is to find the exact probability distribution function (pdf) of the error in the velocity given a known pdf of the error in the signal. We first find analytically the pdf of the phase of the signal, and then by convolution, the pdf of the velocity. These pdfs are different for each pixel.

To confirm the theoretical result, we measured several times the velocity in a simple flow phantom and compared the empirical histogram with the theoretical pdf. We also acquired the velocity from the ascending and descending aorta using a standard protocol for 4D Flow. Finally, we show how our results can be used to estimate the velocity precision, and how that can be used to combine data from multiple coils.

In this manuscript we review the phase contrast technique and we derive the pdf for the velocity (section II); we describe the experiments and finally we show the results (section III) and conclusions (section IV).

II. Theory and Methods

A. MRI Phase-Contrast

For simplicity of notation we will assume two acquisitions, one without velocity encoding m_o, and another with velocity encoding m_1. In practice we can have more encodings and they can occur in other combinations, but the principles are the same. The acquisitions in k-space are:

$$M_o(\mathbf{k}(t)) = \int_{\mathcal{V}} m(\mathbf{x}) e^{-i2\pi \mathbf{k}(t)\cdot\mathbf{x}} d\mathbf{x} \tag{2}$$

and

$$M_1(\mathbf{k}(t)) = \int_{\mathcal{V}} m(\mathbf{x}) e^{-i2\pi (\mathbf{k}(t)\cdot\mathbf{x} + \mathbf{k}_v\cdot\mathbf{v}(\mathbf{x}))} d\mathbf{x}, \tag{3}$$

where $\mathbf{k}(t)$ is the standard k-space trajectory given by the zeroth order moment of the gradients, and $\mathbf{k}_v$ is the first moment of the gradients. It is assumed that the velocity $\mathbf{v}(\mathbf{x})$ is unique for each pixel $\mathbf{x}$ and constant in time. In a noiseless situation the two images would be:

$$m_o(\mathbf{x}) = m(\mathbf{x}) \quad \text{and} \quad m_1(\mathbf{x}) = m(\mathbf{x}) e^{-i2\pi \mathbf{k}_v\cdot\mathbf{v}(\mathbf{x})} \tag{4}$$

ISBN 978-90-827970-1-5 © EURASIP 2018

where m_o and m_1 are the inverse Fourier of M_o and M_1. The velocity is estimated as the difference of the phases:

$$2\pi \mathbf{k}_v \cdot \mathbf{v}(\mathbf{x}) = \phi_o - \phi_1 = \Delta\phi \tag{5}$$

where ϕ and $\Delta\phi$ are in the range $-\pi ... \pi$.

Let $V_{\text{enc}} = 1/(2|\mathbf{k}_v|)$ be the encoding velocity, $v(\mathbf{x}) = \hat{\mathbf{k}}_v \cdot \mathbf{v}(\mathbf{x})$, the projection of the velocity in the direction of the encoding, and $\hat{v}(\mathbf{x}) = v(\mathbf{x})/V_{\text{enc}}$, the velocity in units of V_{enc}, then:

$$\hat{v}(\mathbf{x}) = \frac{\Delta\phi}{\pi}. \tag{6}$$

B. Effect of acquisition noise in the velocity

We assume that the signal acquisition has independent and identically distributed additive Gaussian errors in the real and imaginary channels. To compute the pdf of the velocity, we first derive the pdf of the phase $p_\Phi(\phi)$, and then we compute the auto-convolution (cyclically) to find the pdf of the velocity $p_{\Delta\Phi}(\Delta\phi)$. This is done in a per pixel base, so we drop the dependence of $\mathbf{x}$.

We express the noisy signal as a vector in the complex plane. Without loss of generality we assume that m is real and of magnitude a, such that the measured signal will follow a Gaussian distribution centered in a.

The probability distribution of the angle ϕ will be given by the line integral of the 2D distribution along the direction ϕ, starting from the origin. Let $p_{R,\Phi}(r,\phi)$ be the pdf of the noisy measurement in polar coordinates is:

$$p_{R,\Phi}(r,\phi) = \frac{1}{2\pi\sigma^2} e^{-\frac{r^2 - 2ar\cos\phi + a^2}{2\sigma^2}} \tag{7}$$

which can be solved to be [16], [17]:

$$p_\Phi(\phi) = \frac{1}{2\pi} \left(e^{-b^2} + e^{-b^2\sin^2\phi}\sqrt{\pi} b\cos\phi(1 + \text{erf}(b\cos\phi))\right) \tag{8}$$

where erf is the error function and $b = \frac{1}{\sqrt{2}}(a/\sigma)$. This expression is parameterized to the ratio (a/σ), a quantity related to the signal-to-noise ratio of the original signal. This pdf is plotted in Fig. 1a for different values of b.

For $b = 0$ (no signal) the probability is uniformly distributed in $-\pi \dots \pi$, which can be easily verified in $p_\Phi(\phi)$ since $e^{-b^2} = 1$ and the second term is zero:

$$p_\Phi(\phi) = \frac{1}{2\pi} \tag{9}$$

For larger b (more signal) the pdf tends to a Gaussian distribution. This can be verified by noting $e^{-b^2} \approx 0$, $1 + \text{erf}(b\cos\phi) \approx 2 \sqcap (\frac{\phi}{\pi})$, $\sin\phi \approx \phi$, and $\cos\phi \approx 1$ such that $e^{-b^2\sin^2\phi}\cos\phi \approx e^{-b^2\phi^2}$:

$$p_\Phi(\phi) \approx \frac{b}{\sqrt{\pi}} e^{-b^2\phi^2} \tag{10}$$

which is of course the Gaussian distribution:

$$p_\Phi(\phi) = \frac{1}{\sqrt{2\pi}\sigma_\phi} e^{-\phi^2/2\sigma_\phi^2} \tag{11}$$

with $\sigma_\phi = 1/(\sqrt{2}b) = \sigma/a$.

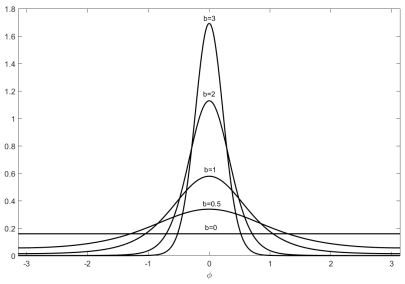

(a) pdf of ϕ

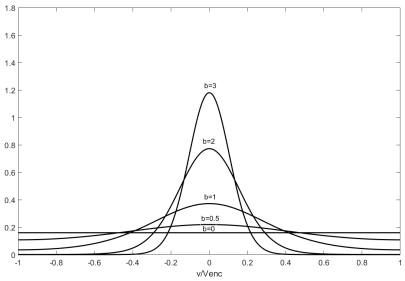

(b) pdf of the velocity ($\Delta\phi/\pi$)

Fig. 1: *Probability distribution of ϕ and $\Delta\phi$ for different values of b.*

Finally, the probability distribution of the velocity (or phase difference) is the auto-convolution of this pdf,

$$p_{\Delta\Phi}(\Delta\phi) = p_\Phi(\phi) \bar{*} p_\Phi(\phi) \tag{12}$$

where $\bar{*}$ is the periodic convolution in the interval $-\pi \dots \pi$. The result of this convolution is shown in Figure 1b for different values of b.

A more practical way for having a notion of the precision of the velocity is to look at its standard deviation and the 68% and 95% intervals (they would correspond to one and two standard deviations if the distribution was Normal). The standard deviation for each b value is shown in Fig. 2a and the intervals in Fig. 2b.

It can be seeing that for b values smaller than 2.5 the Gaussian approximation fails, and that the standard deviation will be overestimated ($b < 0.7$) and slightly underestimated ($0.7 < b < 2.5$).

C. Multiple coils

In a realistic setting, it is common to have data from multiple coils, which are combined using a weighted average.

$$v = \sum_i w_i v_i, \tag{13}$$

The final pdf of the velocity can be expressed as a repeated convolution.

$$p_V(v) = \frac{1}{w_1 \cdots w_N} p_{V_1}(v/w_1) \bar{*} \dots \bar{*} p_{V_N}(v/w_N). \tag{14}$$

Typically, the weights w_i are computed to minimize the final velocity variance ($w = \arg\min \sum_i w_i^2 \sigma_{v_i}^2$). If the pdf of the

ISBN 978-90-827970-1-5 © EURASIP 2018

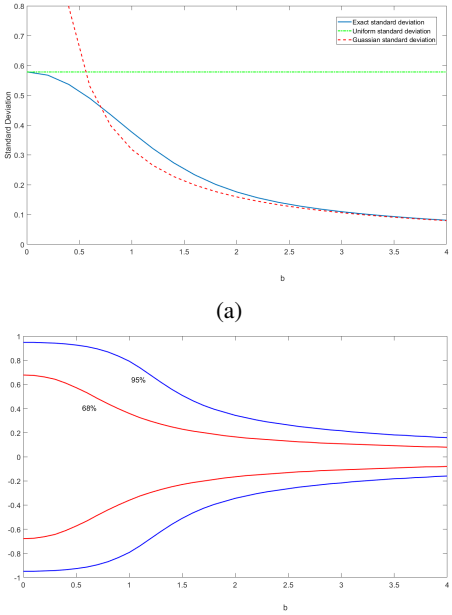

(a)

(b)

Fig. 2: *a) Standard deviation of v/V_{enc} and b) the 68% and 95% interval for v/V_{enc} as a function of b. In (a) we also plot the standard deviation for the uniform and Gaussian distribution.*

velocity were Gaussian, these weights depend only on the coil sensitivities and are [18], [19]:

$$w_i = \frac{S_i^2}{\sum_j S_j^2}. \tag{15}$$

where S_i are the coil sensitivities. We will call this "Gaussian weighting". But for arbitrary variances per coil, it can be calculated that the minimum is achieved for:

$$w_i = \frac{\prod_{j \neq i} \sigma_{v_j}^2}{\sum_k \prod_{j \neq k} \sigma_{v_j}^2}. \tag{16}$$

We propose to use the actual variance as given by Fig. 2a. For this, we need to calculate b. Since we only have one acquisition, we use the weighted average of the coils as an estimation of the magnitude a_i.

$$a_i = S_i |\sum_k S_k m_k| \tag{17}$$

where m_i are the complex images. The sensitivities can be estimated from the same images using low-pass filtering. The signal standard deviation, σ_i can be estimated from background pixels.

D. Experiments

We performed two experiments, in one velocity phantom and in one volunteer. The velocity phantom consisted of a vinyl tubing circuit (12 mm diameter) connected to a water pump which produced a constant water flow of approximately 2.4 l/min and T1=4000ms. The acquisition was done in a 1.5T Philips Achieva scanner employing a 2D Fast Field Echo sequence with TR/TE = 7.1/4.1 ms, resolution of $1.5 \times 1.5 \times 4$ mm^3 and a Venc = 70 cm/s in the trough plane direction with one surface coil. The acquisition was repeated 50 times (with and without velocity encoding) in the exact same conditions. We computed the parameter a as the pixel magnitude averaged over the 50 acquisitions and, σ of the noise as the standard deviation of the real and imaginary components of the signal for the 50 acquisitions.

We also applied our analysis in one volunteer. We scanned separately the ascending and descending aorta to ensure an anatomically perpendicular plane at each location. It was acquired in the same Philips scanner with a five-elements cardiac coil, employing a 4D flow sequence of a single slice with TR/TE = 6.9/4.1 ms for the ascending aorta, TR/TE = 6.9/3.4 ms for the descending aorta, resolution of $1.5 \times 1.5 \times 4$ mm^3, 30 frames per heart beat prospectively gated, and Venc = 200 or 180 cm/s in the ascending and descending aorta respectively.

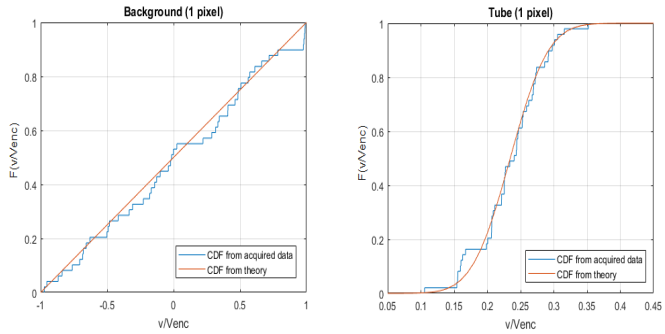

Fig. 3: *Cumulative Distribution Functions (CDF) of the velocity for one pixel in the background and another inside the tube. In blue for the empirical and in red for our theoretical method.*

III. Results and Discussion

A. In-vitro

The phantom data validated our theory. We compared the theoretical pdf with the acquired histogram for pixels in the background and in the tube. Fig. 3 shows the Cumulative Distribution Functions (CDF) for two of these pixels, showing a good fit. Fig. 4 shows the magnitude (a) and velocity (b) for one particular acquisition. Fig. 4c shows the computed values for b and Fig. 4d the standard deviation for the velocity, evaluated from Fig. 2a. We propose to interpret the velocity in the tube as having a "velocity of 35 ± 5 cm/s".

B. In-vivo

We show the results obtained from actual data obtained from the aorta. Fig. 5 shows the values for b, the through plane

ISBN 978-90-827970-1-5 © EURASIP 2018

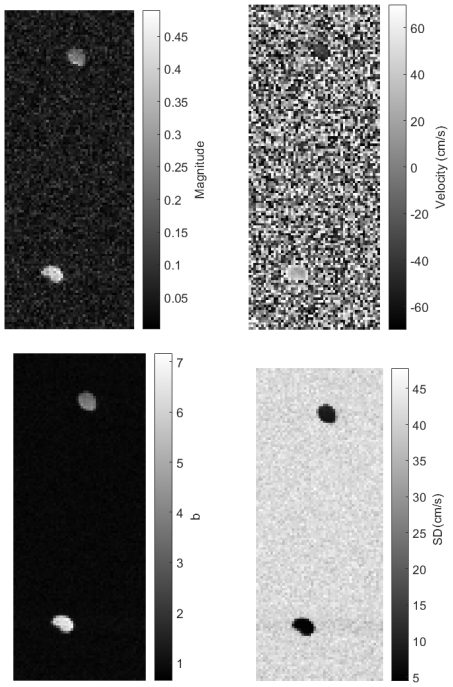

Fig. 4: *Simple velocity phantom: (a) left and top) Magnitude (b) right and top) Phase-contrast velocity in the through plane (c) left and down) b values and (d) right and down) standard deviation (SD) of the velocity.*

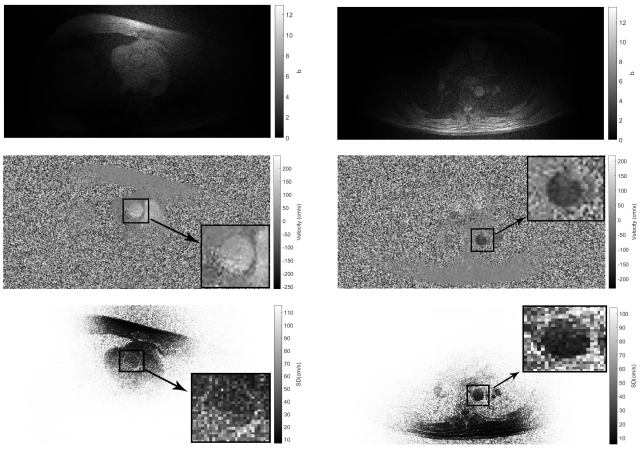

Fig. 5: *Ascending (left) and descending (right) aorta for one particular time frame and one coil, parameter b (first row), velocity (second row) and velocity standard deviation (SD) (third row).*

velocity and the standard deviation of the velocity from the theoretical curve in Fig. 2a. These images correspond to the most relevant coils and the time frame when the velocity is maximum. As expected, the standard deviation of the velocity is larger for low signal regions and farther away from the coil.

We also show the resulting velocity, in Fig. 6, when the coils are combined using the standard Gaussian weighting and

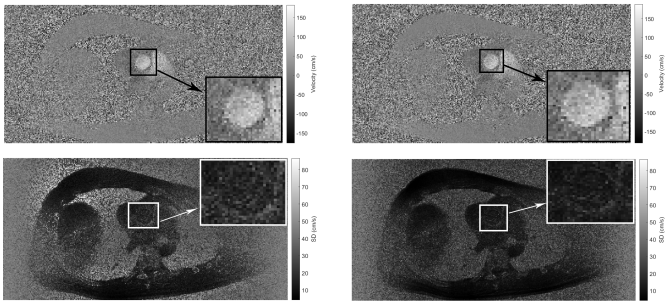

Fig. 6: *Combined velocity (first row) and standard deviation (second row) computed from Gaussian weighting (left) and computed from True pdf weighting (right).*

our proposed True pdf weighting. It can be appreciated that the total variability of the combined velocity is reduced with our proposed weighting. For example, the peak velocity in the ascending aorta changes from 127 ± 17.5 cm/s from the Gaussian weighting to 112 ± 11.8 cm/s from the True pdf weighting.

IV. Conclusion

We formulated a method to obtain the probability density function (pdf) of the velocity in MRI-PC, such that it can be used to estimate the precision in the velocity measurements. We show that this pdf can be approximated to a Gaussian when the voxels are high Signal-to-Noise ratio. The analytical formulation was compared to actual measurements from the scanner showing an excellent fit. In addition, using the correct standard deviation for the velocity in each coil we were able to combine them such that the final velocity variance is minimized.

Acknowledgment

The authors acknowledge financial support from: CONICYT - PIA - Anillo ACT1416, Fondecyt N^o 1181057 and FONDEF project code IT17M10012.

References

[1] D. J. Bryant, J. A. Payne, D. N. Firmin, and D. B. Longmore, "Measurement of flow with NMR imaging using a gradient pulse and phase difference technique," *J Comput Assist Tomogr*, vol. 8, pp. 588–593, Aug 1984.

[2] C. L. Dumoulin, S. P. Souza, M. F. Walker, and W. Wagle, "Three-dimensional phase contrast angiography," *Magnetic Resonance in Medicine*, vol. 9, no. 1, pp. 139–149, 1989.

[3] Z. Stankovic, B. D. Allen, J. Garcia, K. B. Jarvis, and M. Markl, "4D flow imaging with MRI," *Cardiovasc Diagn Ther*, vol. 4, pp. 173–192, Apr 2014.

[4] M. Zhao, F. T. Charbel, N. Alperin, F. Loth, and M. E. Clark, "Improved phase-contrast flow quantification by three-dimensional vessel localization," *Magn Reson Imaging*, vol. 18, pp. 697–706, Jul 2000.

[5] S. Oyre, E. M. Pedersen, S. Ringgaard, P. Boesiger, and W. P. Paaske, "In vivo wall shear stress measured by magnetic resonance velocity mapping in the normal human abdominal aorta," *Eur J Vasc Endovasc Surg*, vol. 13, pp. 263–271, Mar 1997.

[6] P. Papathanasopoulou, S. Zhao, U. Kohler, M. B. Robertson, Q. Long, P. Hoskins, X. Y. Xu, and I. Marshall, "MRI measurement of time-resolved wall shear stress vectors in a carotid bifurcation model, and comparison with CFD predictions," *J Magn Reson Imaging*, vol. 17, pp. 153–162, Feb 2003.

[7] J. M. Tyszka, D. H. Laidlaw, J. W. Asa, and J. M. Silverman, "Three-dimensional, time-resolved (4D) relative pressure mapping using magnetic resonance imaging," *J Magn Reson Imaging*, vol. 12, pp. 321–329, Aug 2000.
[8] G.-Z. Yang, P. J. Kilner, N. B. Wood, S. R. Underwood, and D. N. Firmin, "Computation of flow pressure fields from magnetic resonance velocity mapping," *Magnetic Resonance in Medicine*, vol. 36, no. 4, pp. 520–526, 1996.
[9] A. Nilsson, K. M. Bloch, M. Carlsson, E. Heiberg, and F. Stahlberg, "Variable velocity encoding in a three-dimensional, three-directional phase contrast sequence: Evaluation in phantom and volunteers," *J Magn Reson Imaging*, vol. 36, pp. 1450–1459, Dec 2012.
[10] F. M. Callaghan, R. Kozor, A. G. Sherrah, M. Vallely, D. Celermajer, G. A. Figtree, and S. M. Grieve, "Use of multi-velocity encoding 4D flow MRI to improve quantification of flow patterns in the aorta," *J Magn Reson Imaging*, vol. 43, pp. 352–363, Feb 2016.
[11] S. Ringgaard, S. A. Oyre, and E. M. Pedersen, "Arterial MR imaging phase-contrast flow measurement: improvements with varying velocity sensitivity during cardiac cycle," *Radiology*, vol. 232, pp. 289–294, Jul 2004.
[12] N. J. Pelc, R. J. Herfkens, A. Shimakawa, and D. R. Enzmann, "Phase contrast cine magnetic resonance imaging," *Magn Reson Q*, vol. 7, pp. 229–254, Oct 1991.
[13] N. J. Pelc, M. A. Bernstein, A. Shimakawa, and G. H. Glover, "Encoding strategies for three-direction phase-contrast MR imaging of flow," *J Magn Reson Imaging*, vol. 1, no. 4, pp. 405–413, 1991.
[14] T. E. Conturo and G. D. Smith, "Signal-to-noise in phase angle reconstruction: Dynamic range extension using phase reference offsets," *Magnetic Resonance in Medicine*, vol. 15, no. 3, pp. 420–437, 1990.
[15] A. H. Andersen and J. E. Kirsch, "Analysis of noise in phase contrast mr imaging," *Medical Physics*, vol. 23, no. 6, pp. 857–869, 1996.
[16] W. B.jun. Davenport and W. L. Root, "An introduction to the theory of random signals and noise," vol. 11, p. 167, 01 1958.
[17] H. Gudbjartsson and S. Patz, "The Rician distribution of noisy MRI data," *Magn Reson Med*, vol. 34, pp. 910–914, Dec 1995.
[18] M. Bydder, D. J. Larkman, and J. V. Hajnal, "Combination of signals from array coils using image-based estimation of coil sensitivity profiles," *Magn Reson Med*, vol. 47, pp. 539–548, Mar 2002.
[19] P. Thunberg, M. Karlsson, and L. Wigstrom, "Comparison of different methods for combining phase-contrast images obtained with multiple coils," *Magn Reson Imaging*, vol. 23, pp. 795–799, Sep 2005.

ISBN 978-90-827970-1-5